

# Kinetics of thermal decomposition of hydroxyapatite bioceramics

J. CIHLÁŘ, A. BUCHAL, M. TRUNEC

*Department of Ceramics, Institute of Materials Engineering, Technical University of Brno, Technická 2, 616 69 Brno, Czech Republic*

*E-mail: cihlar@ro.vutbr.cz*

The mechanism and kinetics of thermal decomposition of injection moulded hydroxyapatite ceramics were studied over the temperature range of 1473–1758 K. At temperatures below 1473 K the sintering and transformation of hydroxyapatite to hydroxyoxyapatite proceeded to a conversion degree of 0.4 to 0.5. At temperatures between 1473 and 1758 K the hydroxyapatite was decomposed to  $\alpha$ -TCP, H<sub>2</sub>O and CaO. The decomposition of HOA started on the surface of the HOA ceramics. The rate of increase in the thickness of the reaction products ( $\alpha$ -TCP) was described by the parabolic law. The kinetic analysis of the time dependence of HOA conversion to TCP by means of the J-M-A-J-K equation also showed that the thermal decomposition of HOA ceramics was controlled by diffusion of water from the reaction zone to the surface of the ceramic sample. The activation energy of the thermal decomposition of HOA ceramics amounted to 283.5 kJ/mol. © 1999 Kluwer Academic Publishers

## 1. Introduction

Thermal decomposition of hydroxyapatite (HA) taking place during the sintering of HA ceramics or during application of HA coatings affects the physical, mechanical, chemical as well as biological properties of HA ceramics and coatings.

The decomposition of HA proceeds in two stages: reversible expulsion of water producing oxyapatite (OA), and irreversible decomposition to HA yielding calcium phosphates. Whereas the first decomposition stage has no significant effect on the properties of HA ceramics, the other leads to impairing the mechanical properties [1, 2], to higher chemical activity [3] and to poorer stability of HA in the organism [4]. Water and powdered HA begin to be separated already at 1173 K. The water is liberated gradually, and hydroxyoxyapatite  $\text{Ca}_{10}(\text{PO}_4)_x(\text{OH})_{2(1-x)}$  (HOA) with a gradually decreasing content of OH groups is formed.

This process can be observed by IR spectroscopy [5]. A mild shift of the lattice parameters towards lower values occurs [5, 6] in the course of water separation. However, the changes are small and of no practical use for describing quantitatively the HA-OA conversion. Data in the literature concerning the other stage of HA (or HOA) decomposition are not unambiguous as regards the minimum decomposition temperature, as well as the actual decomposition mechanism. This is most frequently described by the summary equation  $\text{HA} \rightarrow 2\text{TCP} + \text{TetCP} + \text{H}_2\text{O}$  (TCP—tricalcium phosphate, TetCP—tetracalcium phosphate) [7, 8, 9, 10]. The initial decomposition temperature is variously specified at 1323 K [7], or 1573 K [8, 9] or even 1750 K [10].

The differences in the minimum temperature of decomposition of HA, or those in the explanation of the decomposition mechanism, were probably associated with the purity of HA, the powdered form of HA and the conditions under which the decomposition was studied. A significant role was obviously played by water vapour pressure in the furnace atmosphere. The decomposition temperature of HA increased with increasing water vapour pressure [11].

The available information from the literature described the decomposition of HA from a qualitative point of view. The present study is concerned with a qualitative (semiquantitative) kinetic description of the thermal decomposition of hydroxyapatite ceramics.

## 2. Experimental

### 2.1. Preparation of samples

The samples of HA ceramics were prepared by powder injection moulding of HA powder supplied by Riedel de Haën (Seelze, Germany). ICP analysis of HA powder: Ca/P molar ratio 1.669; Pb 45.0 ppm; As 1.0 ppm; Ba 81.0 ppm; Mg 52.0 ppm and Fe 39.0 ppm. The other materials employed and the actual preparation are described in [1]. The HA ceramics were heat treated under isothermal conditions in air atmosphere at a relative humidity of 25 rel.%. The isothermal temperature over the range of 1573–1773 K was held for periods ranging from 0.5–22 h. Following the thermal exposure, the sintered samples were crushed and ground to powder of 10 to 50  $\mu\text{m}$  particle size and analysed by X-ray phase analysis.

Apart from samples of HA prepared by injection moulding, the thermal decomposition of HA was also studied on powdered samples. Use was made of the same hydroxyapatite (Riedel-de-Haën) as for the injection moulding. The powdered HA was heat treated under the same conditions as the injection moulded samples.

## 2.2. X-ray diffraction analysis

The powdered samples were analyzed on the D500 diffractometer in Bragg-Bretano arrangement by radiation  $\text{FeK}\alpha$  ( $\lambda_{\text{K}\alpha 1} = 0.193597$  nm, and  $\lambda_{\text{K}\alpha 2} = 0.193991$  nm). The X-ray diffraction spectrum region was measured from  $10^\circ 2\theta$  up to  $90^\circ 2\theta$  by steps of  $0.05^\circ 2\theta$  by holding 39 s in each position. The spectra were measured in a standard way using a  $1^\circ$  divergence of the primary beam, with the sample rotating at the goniometer axis and a 0.15 mm diaphragm in front of the scintillation detector.

The qualitative phase analysis of the samples was based on comparing the spectra measured with the PDF1-ICDO-JCPDS database [11]. Two phases were essentially identified in the diffraction patterns, namely hydroxyapatite and  $\alpha$ -TCP (cf. Fig. 1). Thermogravimetric analysis revealed a weight loss due to water expelled from HA already at 1173 K. For this reason the hydroxyapatite phase has been designated hydroxyapatite, HOA. Two problems were dealt with in the quantitative determination of the identified phases:

1. precise determination of the intensities for the individual systems of crystal planes,
2. assignment of concentrations to the intensities measured.

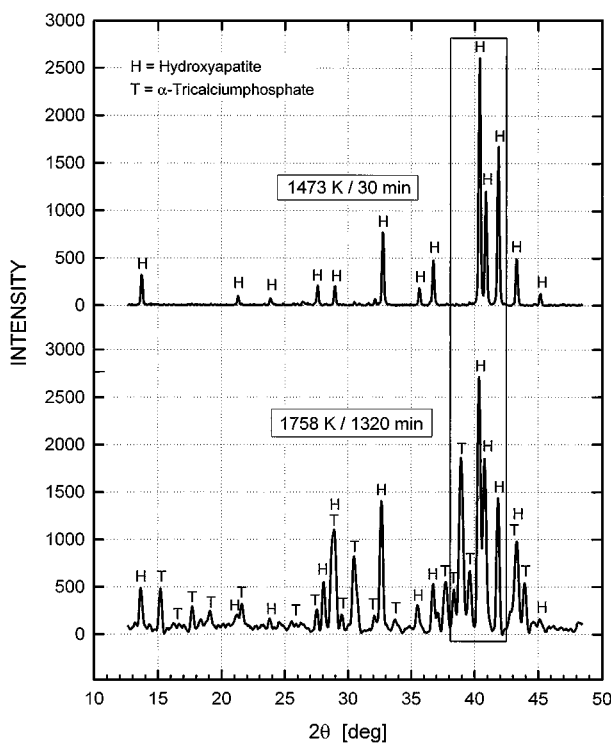


Figure 1 X-ray spectrum of injection moulded HA ceramics in terms of temperature and time of heat treatment (sintering).

The first problem was solved by substituting the intensity function measured by the final sum of Lorenz-type functions so as to obtain the minimum sum of squared deviations of the measured and calculated values. In function 1,

$$I(x) = \frac{\text{height}}{\left[1 + Q \cdot \left(\frac{x - \text{position}}{\text{breadth}}\right)^2\right]^2} + \frac{0.497 \cdot \text{height}}{\left[1 + Q \cdot \left(\frac{x - \text{position} - \Delta}{\text{breadth}}\right)^2\right]^2} \quad (1)$$

$$\Delta = \arcsin \left\{ \frac{\lambda \bar{K}_{\alpha 2}}{\lambda \bar{K}_{\alpha 1}} \cdot \sin(\text{position}) \right\} - \text{position} \quad (2)$$

$$Q = 4 \cdot (\sqrt{2} - 1) \quad (3)$$

where  $Q$  was chosen so as to make the height  $\times$  breadth product equal to the integral intensity.

In this way it was possible to separate even the mutually overlapping diffractions and to determine their integral intensities with relative accuracy. The result of the procedure is shown in Fig. 2 which depicts the parts of the diffraction spectrum employed in the quantitative analysis, and the Miller's indices of diffraction planes of the two phases present in the samples, hydroxyapatite and  $\alpha$ -TCP.

The other problem was solved by means of standard samples containing known amounts of hydroxyapatite and TCP. The quantitative phase analysis was based on Klug-Alexander's relation rearranged into the form 4 [12],

$$J_{\text{HA}}^{hkl} = \frac{K_{\text{HA}}^{hkl} \cdot c_{\text{HA}}}{\mu_{\text{spec}}^*} = I_{\text{HA}}^{hkl} \cdot c_{\text{HA}} \quad (4)$$

where

$J_{\text{HA}}^{hkl}$  is the intensity of the hydroxyapatite system of planes,

$I_{\text{HA}}^{hkl}$  is the intensity of the hydroxyapatite system of planes, corrected for sample absorption,

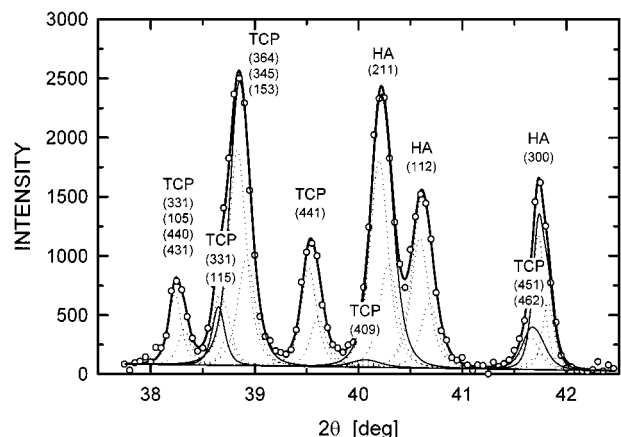


Figure 2 Separation of X-ray diffractions used in quantitative analysis.

$\mu_{\text{spec}}^*$  is the absorption coefficient of the sample, and  $c_{\text{HA}}$  is the concentration of hydroxyapatite.

The problems involved in the determination of the absorption coefficient of the sample were resolved by measuring  $I_{\text{HA}}$  and  $I_{\text{TCP}}$  on standard samples containing known amounts of HA and TCP. The intensities of selected diffractions of HA ( $I_{\text{HA}}$ ) and TCP ( $I_{\text{TCP}}$ ) were expressed in dimensionless form as  $I_{\text{HA}}/(I_{\text{HA}} + I_{\text{TCP}})$  and  $I_{\text{TCP}}/(I_{\text{HA}} + I_{\text{TCP}})$  and plotted in calibration curves in terms of HA or TCP content in the standard samples.

The amount of HA in the analyzed sample (in weight fractions),  $x_{\text{HA}}$ , was calculated by means of Equation 5:

$$\frac{I_{\text{HA}}}{I_{\text{HA}} + I_{\text{TCP}}} = \frac{I_{\text{HA}}}{I_{\text{celk}}} = -0,0049 + 1,9952x_{\text{HA}} - 0,9939x_{\text{HA}}^2 \quad (5)$$

This quantitative phase analysis procedure holds on the assumptions that only two phases HA (or HOA) and  $\alpha$ -TCP are present in the sample being analyzed, that the sample weight does not change during thermal exposure, and that no amorphous Ca/P phases are formed during the HA  $\rightarrow$  TCP conversion.

### 2.3. Testing of the samples

The microstructure of the sintered injection-moulded samples was studied and analyzed by the JXA-840 microscope (Jeol) using the AN 10000 microanalyzer (Link). The thermogravimetric changes in the samples of HOA ceramics were studied in air atmosphere in a superkanthal furnace (Heraeus) under isothermal conditions at the respective temperatures of 1473, 1573, 1623, 1673, 1723 and 1758 K for periods ranging from 0.5 to 22 h, and by means of the thermal analyzer Derivatograph Q1500D (MOM). The composition of the gaseous phase escaping from the furnace was studied by gas chromatography (Chrom5, Laboratory Equipments).

### 2.4. Kinetic processing of analytical data

The experimentally established values of concentrations of HA or HOA and TCP ( $x_{\text{HOA}}$ ,  $x_{\text{TCP}}$ ), obtained by means of quantitative diffraction phase analysis, were recalculated to the degree of HOA conversion by means of Equation 6,

$$\alpha_{\text{HOA}} = \frac{(x_{\text{HOA}})_0 - (x_{\text{HOA}})_t}{(x_{\text{HOA}})_0}, \quad (6)$$

where

$(x_{\text{HOA}})_0$  is the concentration of HOA in sample at the onset,

$(x_{\text{HOA}})_t$  is the concentration of HOA in sample at time  $t$ ,

$\alpha_{\text{HOA}}$  is the degree of conversion of HOA at time  $t$ .

In the kinetic processing of experimental data and in describing the thermal decomposition of HOA, use was made of the general Johanson-Mehl-Avrami-Jerofyeev-Kolgomorov's (J-M-A-J-K) Equation 7, [13, 14, 15]

$$-\ln(1 - \alpha_{\text{HOA}}) = k \cdot t^m, \quad (7)$$

where

$k$  is the overall rate constant of the process,

$m$  is the exponent factor.

For graphic processing of the kinetic data, Equation 7 was converted to its logarithmic form 8,

$$\ln(-\ln(1 - \alpha_{\text{HOA}})) = \ln k + m \ln t \quad (8)$$

The activation energy of thermal decomposition of HOA was evaluated by means of Arrhenius' Equation 9,

$$\ln k = \ln A - \frac{E}{RT}, \quad (9)$$

where

$A$  is the pre-exponential factor,

$E$  is the activation energy.

The increase in the thickness of the products of HOA thermal decomposition in terms of time was described by Equation 10, [16]

$$x = (D \cdot t)^{1/2}, \quad (10)$$

where

$D$  is the diffusion coefficient

$x$  is the layer thickness [ $\mu\text{m}$ ].

The loss in weight of samples after thermal exposure was expressed as conversion of water ( $\alpha_{\text{H}_2\text{O}}$ ) by means of Equation 11,

$$\alpha_{\text{H}_2\text{O}} = \frac{g_0 - g_t}{g_0 - g_\infty}, \quad (11)$$

where

$g_0$  is the sample weight before thermal exposure,

$g_t$  is the sample weight at time  $t$ , and

$g_\infty$  is the sample weight at total (theoretical) conversion of water.

## 3. Results

### 3.1. Thermal decomposition of injection-moulded hydroxyapatite

The course of hydroxyapatite (HA) conversion in terms of time and temperature of sintering is plotted in Fig. 3. A single crystalline phase, hydroxyapatite, was determined at 1573 K. In the course of thermal exposure, the diffractions were slightly shifted (by about  $0.2^\circ$ ) towards higher values. This change in the diffraction spectrum was probably caused by gradual conversion of hydroxyapatite to hydroxyoxyapatite (HOA) [5, 6].

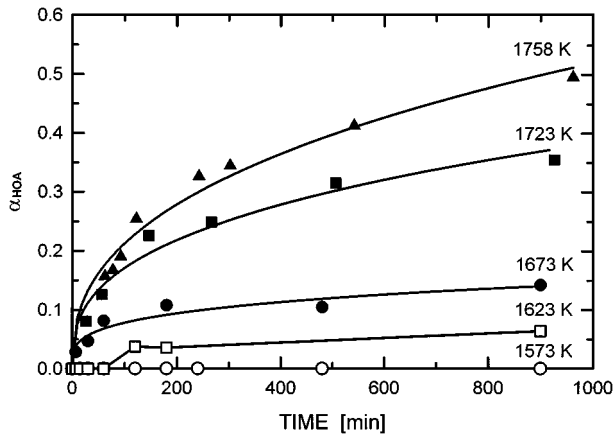


Figure 3 Conversion of HOA in terms of time and temperature of sintering of injection moulded hydroxyapatite ceramics.

This conversion was accompanied by liberation of water which started at about 1173 K. The thermal decomposition of HOA producing TCP was detected at temperatures as high as 1623 K. The degree of HOA conversion was low, attaining the value of 0.6 after 900 min of sintering. The kinetics of thermal decomposition of HOA was studied over the range of 1673 to 1758 K where the conversion degree was adequately high. The conversion degree in terms of time, expressed by the J-M-A-J-K Equation 8, is plotted in Fig. 4. Table I shows that the correlation coefficients ( $R^2$ ) of  $\ln\{-\ln(1 - \alpha)\}$  vs.  $\ln t$  were within the range of 0.95 to 0.97. The exponent factor  $n$  had values ranging

TABLE I Kinetic parameters of thermal decomposition of hydroxyapatite

Hydroxyapatite	Temperature [K]	$\ln k$	$k \cdot 10^2$ [ $s^{-1}$ ]	$m$	$R^2$	$E$ [kJ/mol]
Injection moulded	1673	-4.81	0.82	0.53	0.97	
	1723	-4.10	1.67	0.50	0.95	283.5
	1758	-3.84	2.15	0.51	0.97	
Powder	1673	-3.47	3.11	0.65	0.93	
	1723	-2.74	6.46	0.59	0.99	300.2
	1758	-2.44	8.72	0.59	0.95	

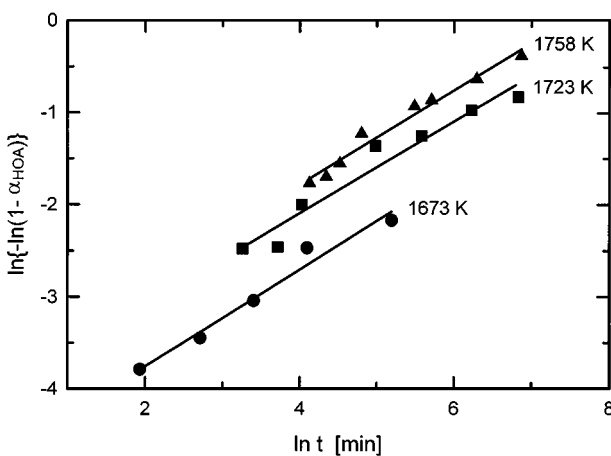


Figure 4 Conversion of HOA in terms of time and temperature of sintering of injection moulded hydroxyapatite ceramics (Johanson-Mehl-Avrami-Jerofyeev-Kolgomorov's equation).

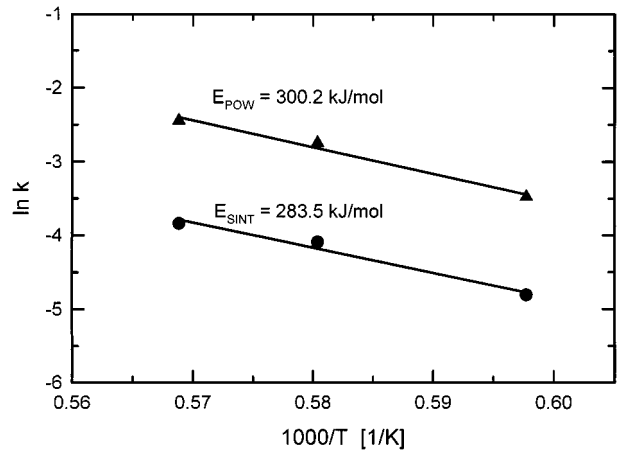
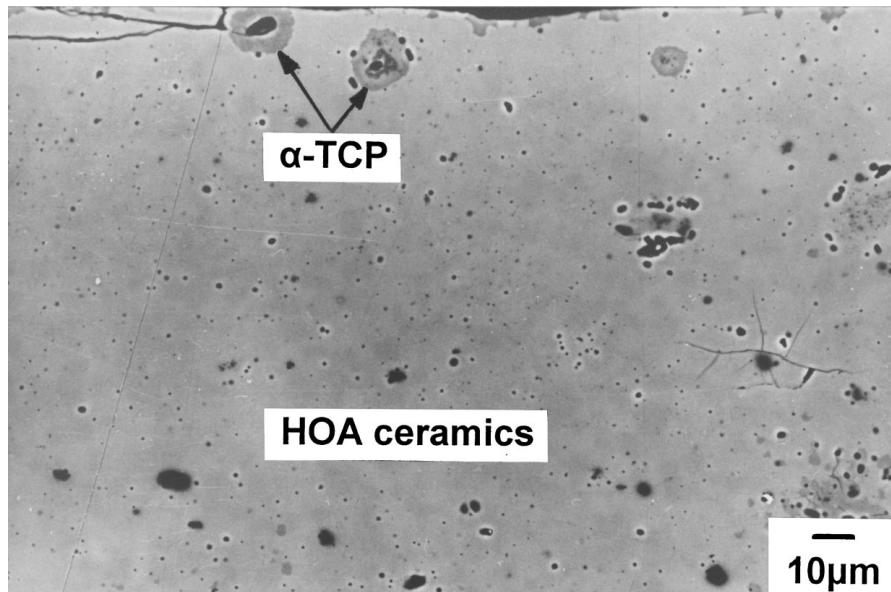


Figure 5 Temperature dependence of the rate constant of HOA thermal decomposition: Sint—sintered HOA; Pow—powdered HOA.

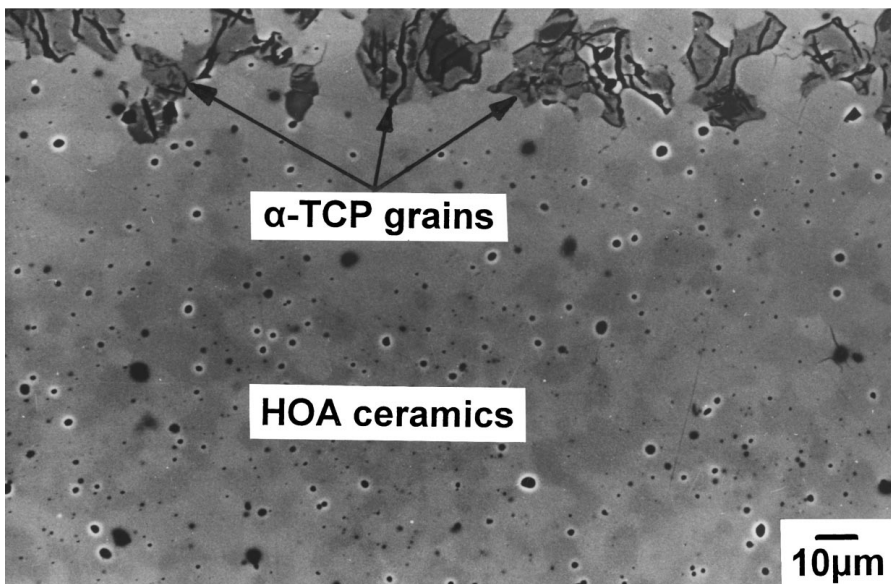
from 0.5 to 0.53. The overall rate constant was increasing with increasing temperature from  $8.15 \times 10^{-3} s^{-1}$  (1673 K) up to  $2.15 \times 10^{-2} s^{-1}$  (1758 K). The temperature dependence of the overall rate constant is plotted in Fig. 5. The activation energy of thermal decomposition of injection-moulded HOA had the value of 283.5 kJ/mol. The sequence of thermal decomposition of sintered HOA is illustrated by Figs 6A–6F. The decomposition started on the sample surface and in the proximity of pores close to the surface (Fig. 6A). During the subsequent stage of HOA decomposition, the separated grains of the decomposition product (Fig. 6B) fused into a compact layer (Fig. 6C). The thickness of the decomposition product increased with time and temperature (Figs 6D–F). The structure of the layer of decomposition product was different from that of HAO ceramics (Figs 6G and H). The results of the microanalysis (the sample given on the Fig. 6E) are plotted in Fig. 7. The Ca/P molar ratio ranged from 1.5 to 1.52 in dependence on the distance from the surface (the layer of the decomposition product), and from 1.65 to 1.7 (in the sample interior). The Ca/P molar ratio of 1.5 corresponded to tricalcium phosphate (TCP), the Ca/P molar ratio of 1.67 to hydroxyapatite. Both phases were confirmed by X-ray analysis. The dependence of TCP layer thickness on the time of sintering is plotted in Fig. 8. A comparison of the experimental course with the theoretical diffusion model of product layer growth exhibits a satisfactory agreement for longer times of sintering (correlation coefficient  $R^2 = 0.97$ ).

In the course of sintering the weight of the samples being sintered decreased as a result of water removal (Fig. 9). Over the temperature range of 1473–1623 K, the water conversion attained rapidly the value of 0.42 to 0.47 at the onset of sintering, and subsequently remained virtually unchanged. With sintering temperatures above 1623 K the water conversion value rose very rapidly to 0.42–0.48, and then increased at a lower rate. The maximum water conversion of 0.93 was attained at 1758 K within 986 min.

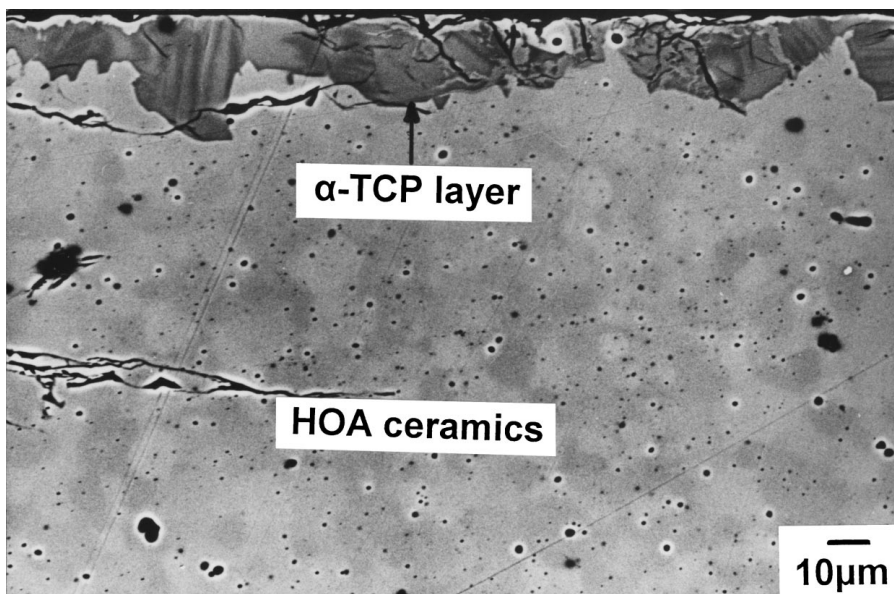
The two stages of water releasing rate were probably associated with the density of the samples being sintered. Fig. 10 shows the dependence of volume shrinkage on the time of sintering. The diagram indicates that



(A)

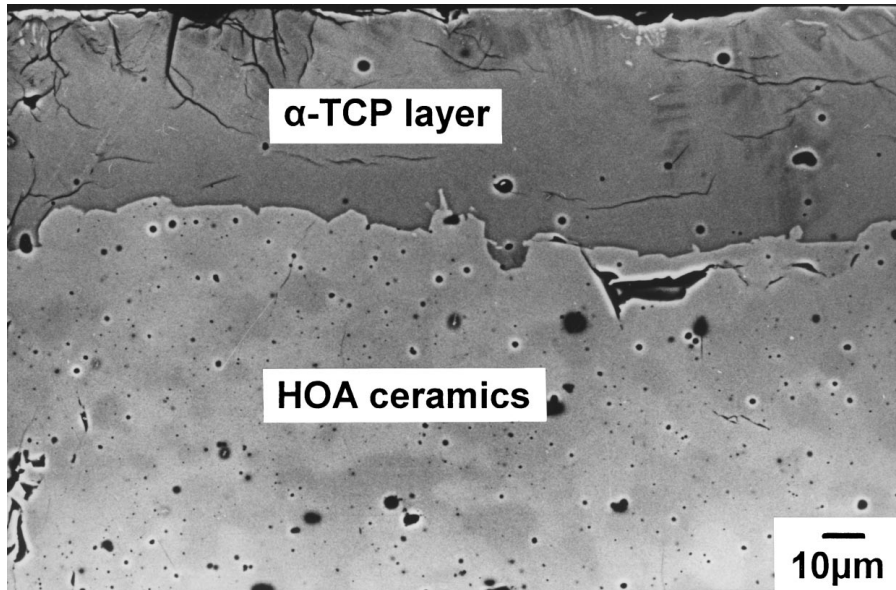


(B)

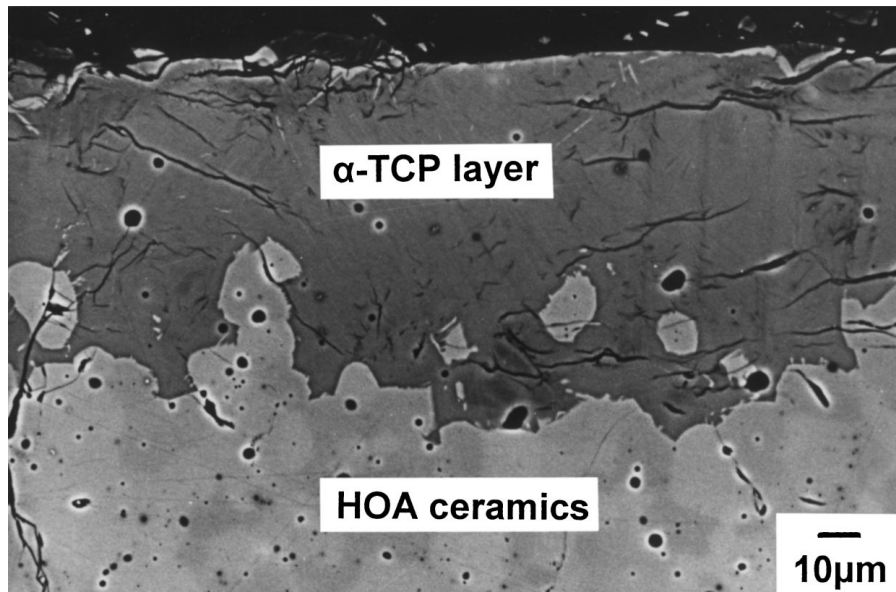


(C)

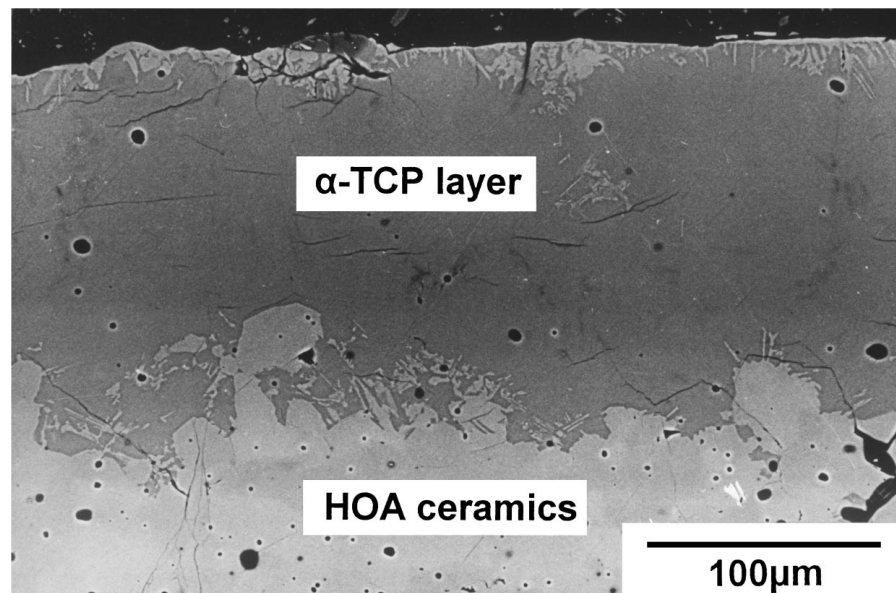
Figure 6 Microstructure of injection-moulded hydroxyapatite ceramics, sectional view A—1573 K/2 h, B—1573 K/22 h, C—1673 K/2 h, D—1673 K/4 h, E—1673 K/8 h, F—1673 K/22 h, G—the layer of decomposition product (etched by acetic acid), H—HOA ceramics (etched by acetic acid) (Continued)



(D)

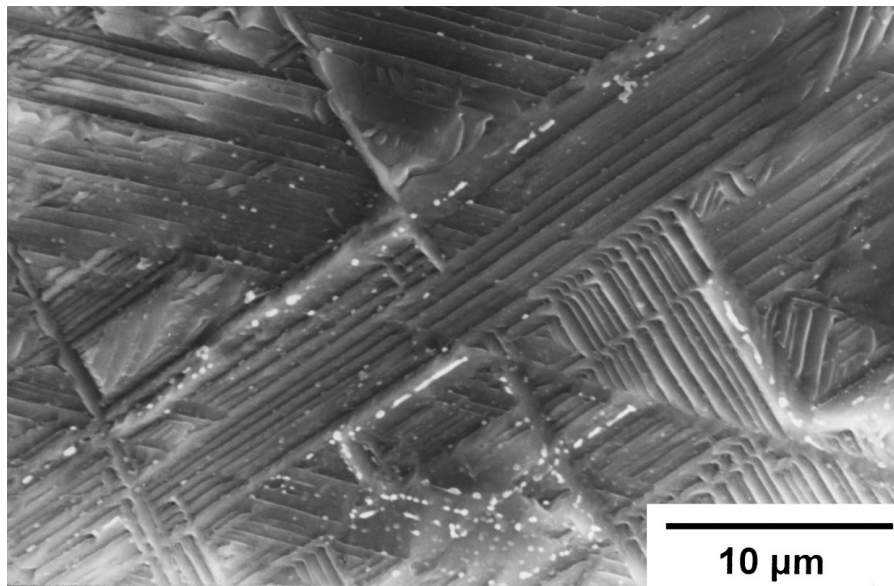


(E)

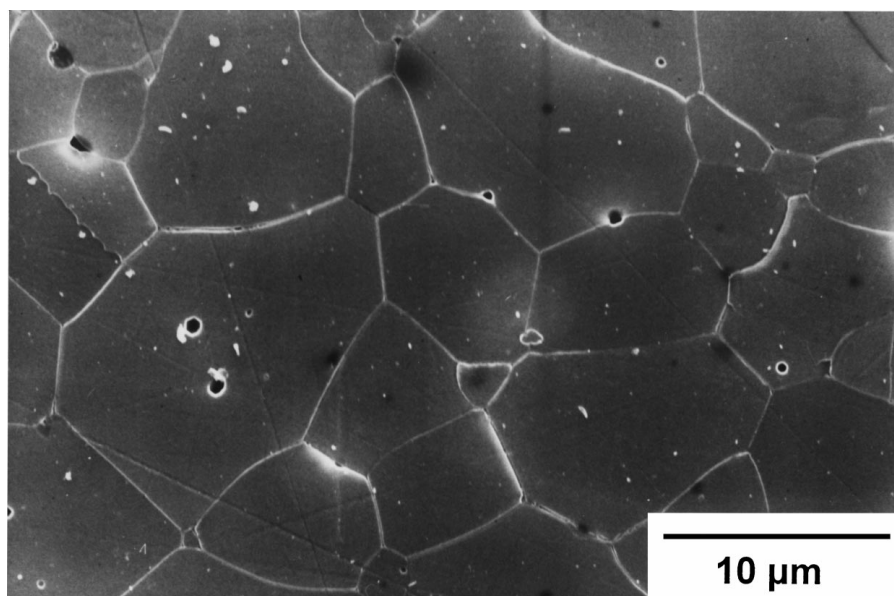


(F)

Figure 6 (Continued)



(G)



(H)

Figure 6 (Continued).

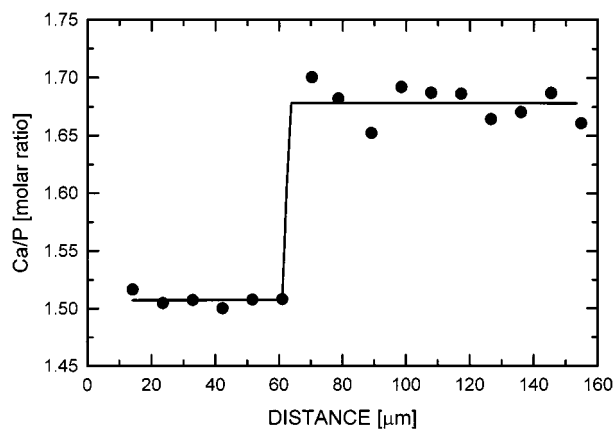


Figure 7 Molar ratio Ca/P vs. distance from surface of hydroxyapatite ceramics sintered at 1673 K/8 h (sample 6E, Fig. 6).

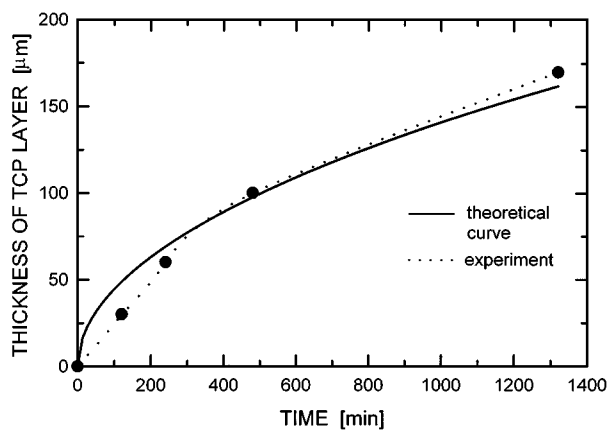


Figure 8 Thickness of  $\alpha$ -TCP layer vs. time of sintering (sintering temperature 1758 K).

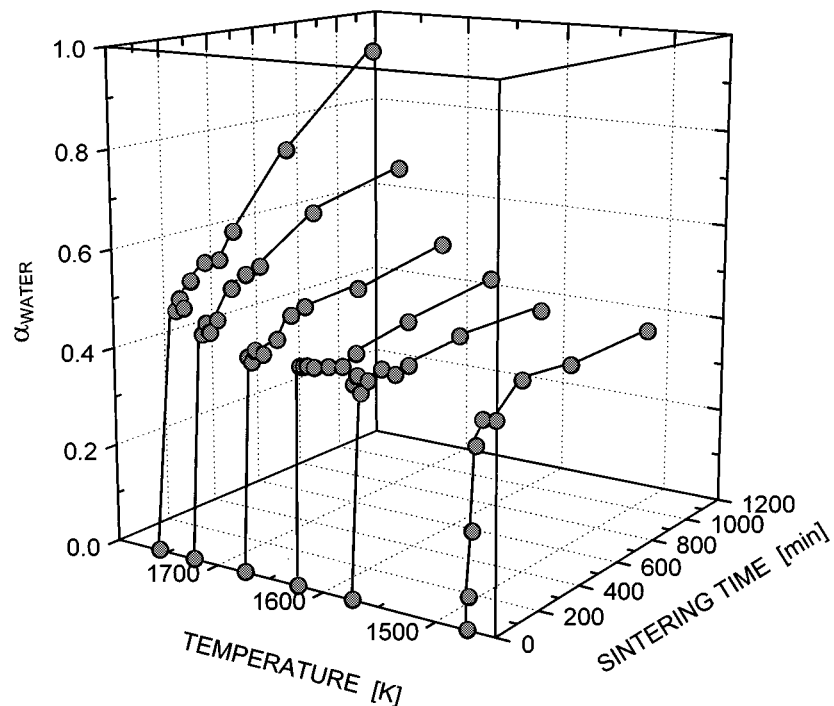


Figure 9 Conversion of water vs. temperature and time of sintering of injection moulded hydroxyapatite ceramics.

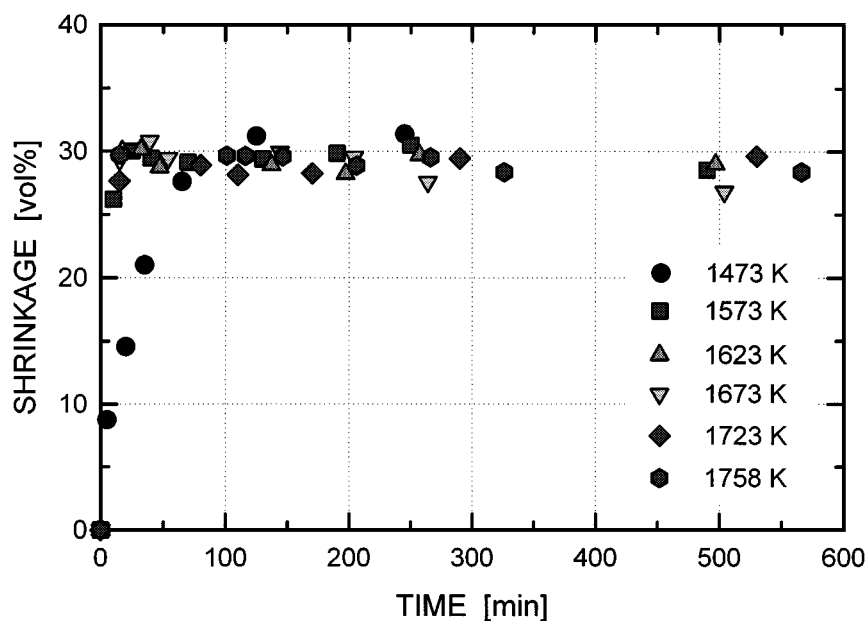


Figure 10 Volume shrinkage of injection moulded hydroxyapatite ceramics vs. temperature and time of heat treatment.

the sintered samples had a maximum volume shrinkage of about 30%. A comparison of Figs 9 and 10 show that the greatest loss of water occurred during the initial stage of sintering before the maximum density of HOA ceramics was attained.

The relation between conversion of HOA to TCP and the water conversion is plotted in Fig. 11. No relationship was found between water removal and formation of TCP during the initial stage of thermal conversion of HOA. In the initial stage the conversion of water reached about 40%. During the second stage of the process, when the sintered samples underwent thermal decomposition, the water conversion was increasing jointly with that of HOA to  $\alpha$ -TCP. The correlation between conversion of water and that of HOA was sig-

nificant, in particular with samples heat treated at 1673 and 1758 K.

### 3.2. Thermal decomposition of powdered hydroxyapatite

The course of HOA conversion in terms of time and temperature is plotted in Fig. 12. Similar to the case of sintered HOA, the decomposition product TCP was detected at temperatures above 1573 K. The kinetic dependence of HOA conversion on the time of reaction, described by the J-M-A-J-K equation, is shown in Fig. 13. The values of the overall rate constant of thermal decomposition of powdered HOA are listed in Table I. The value of exponent  $n$  was in the range of 0.59 to 0.65.



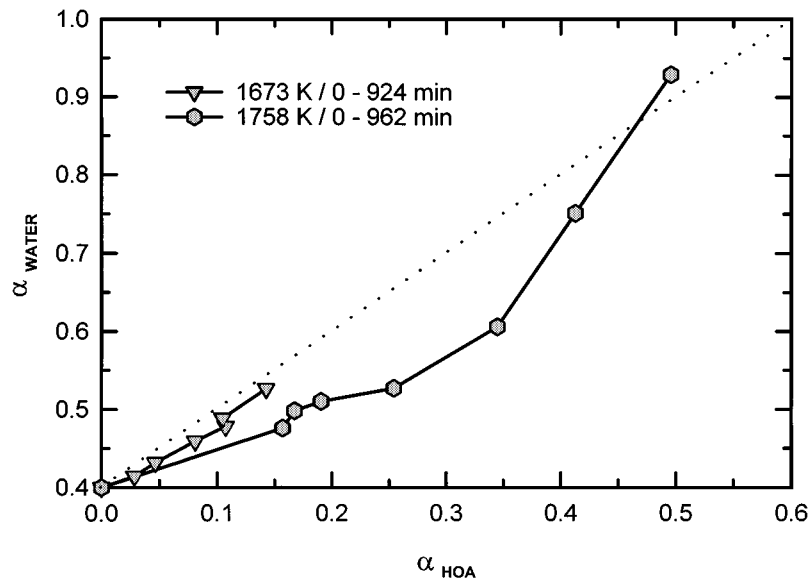


Figure 11 Relation between conversion of HOA and conversion of water for injection moulded HA ceramic material.

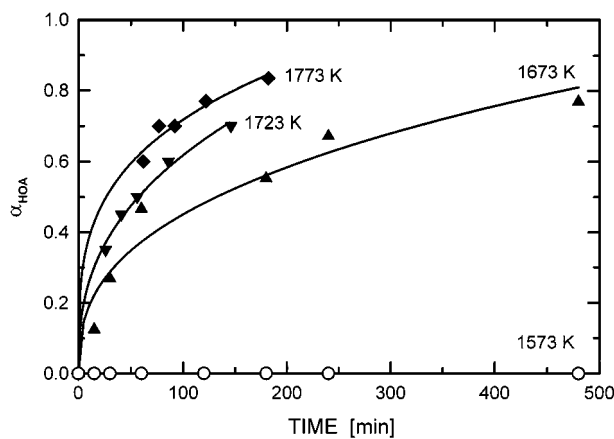


Figure 12 Conversion of HOA vs. time and temperature of heat treatment of powdered HA.

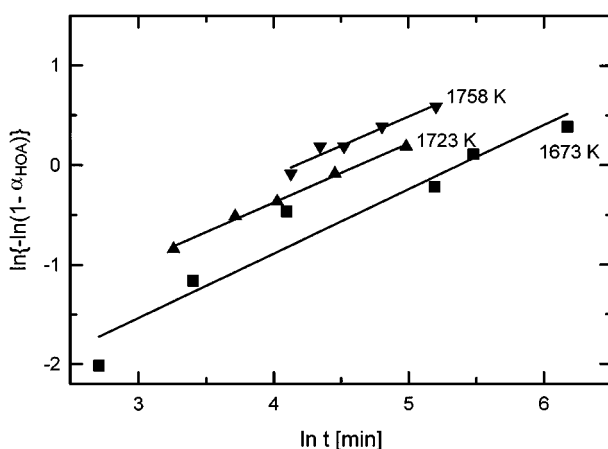


Figure 13 Conversion of HOA vs. time and temperature of heat treatment of powdered HA (J-M-A-J-K equation).

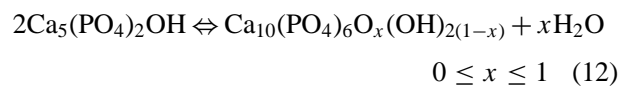
On the basis of the temperature dependence of the rate constant shown in Fig. 5 the activation energy of decomposition of powdered HOA had the value of 300.2 kJ/mol.

#### 4. Discussion

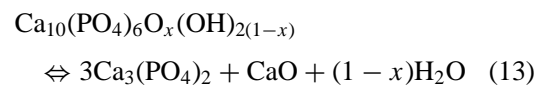
The results of X-ray diffraction analysis, thermogravimetry and gas chromatography showed that over the temperature interval studied, between 1473 and 1758 K, hydroxyapatite is decomposed while releasing water and producing tricalcium phosphate. The first water was expelled at above 1173 K and the dewatering proceeded even at 1758 K (a conversion degree of about 0.9 being attained at the latter temperature).

The onset of hydroxyapatite decomposition yielding TCP was detected at 1623 K. Diffractions of tetracalcium phosphate appeared at about 1773 K. On the basis of the results obtained, the following scheme of thermal decomposition of HA ceramics for the temperature interval of 1173 to 1758 K was proposed:

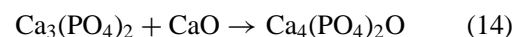
$$1173 - 1623 \text{ K}$$



$$1623 - 1758 \text{ K}$$



TetCP started to form at temperatures above 1750 K according to the equation



The first equation of the scheme, describing conversion of HA to HOA and liberation of water, was examined thermogravimetrically. No significant differences were established between the diffraction spectra of HA and HOA.

The second equation of the scheme, describing the thermal decomposition of HOA to  $\alpha$ -TCP and CaO, is based on the results of diffraction analysis. Diffraction lines of two crystalline phases, HOA and  $\alpha$ -TCP, were found in the spectra within the temperature range of 1623 to 1758 K. No diffractions of CaO were found,

probably owing to the low concentration and amorphous structure of CaO.

At 50% conversion of HOA (the highest attained one), 3.7% CaO were formed. The presence of CaO in the reaction products of HOA decomposition was not taken into account in the preparation of standard solutions for quantitative analysis.

However, the error introduced into the determination of HA conversion by this simplification did not exceed 5% (at the maximum 50% conversion of HA).

On comparing the proposed scheme of thermal decomposition of sintered HA with data from the literature one sees that the proposed scheme differs from most of the data in the proposed mechanism of formation of TetCP, and in the initial temperature of TCP and TetCP formation.

Whereas numerous authors [7, 8, 9] stated that the onset of decomposition of HA to TCP and TetCP occurred at the same temperature, in our case and under all conditions the formation of TetCP was confirmed to take place at temperatures higher by at least 130 K than the formation of TCP (1623 vs. >1758 K). The minimum temperature of TCP established by the present authors (1623 K) does not likewise agree exactly with the literary data (cf. the Introduction). We assume that the differences are due to a different arrangement of our experiments (kinetic study of decomposition of HA ceramics), to the purity of reagents and to water vapour content in the furnace atmosphere.

The mechanism of thermal decomposition of HA ceramics involves four processes: sintering, removal of water, decomposition of HA to TCP, and formation of TetCP. The sintering caused the HA ceramics to shrink by at least 30 vol.%. On neglecting the fact that thermal exposure changes the composition of HA ceramics, the 30% shrinkage would correspond to a relative density of about 0.93. During sintering, the "open" porous structure was transformed into a sintered one with closed pores. The time required for maximum shrinkage and closing of pores in HA ceramics was decreasing with increasing temperature.

At 1473 K the closed structure formed within 75 min, at 1573 K within 30 min, and at temperatures above 1573 K within less than 30 min. The liberation of water associated with conversion of HA to HOA proceeded in one or two stages. At 1473, 1573 and 1623 K this process took place in one stage. The maximum conversion of water was within the range of 0.4–0.5. At 1473 K, the maximum conversion of water was attained within 75 min, at 1573 K within 30 min, and at 1623 K within 15 min.

As soon as the maximum conversion was attained, the decomposition stopped and the HA (or HOA) ceramic material showed a long-term stability (for up to 90 min). This rapid expulsion of water proceeded during the time the porosity was still open and stopped as soon as the pores in the HA ceramic material closed. At temperatures of 1673, 1723 and 1758 K the water was separating from HA in two stages differing in the rate of the process. During the first stage, i.e. that with the pores still open, 40 to 50% of the water escaped rapidly within 10 min.

As soon as the HA ceramic material has sintered and its pores closed, the rate of water releasing slowed down but did not stop completely. This second stage was observed at temperatures equal to, and higher than, 1673 K. It was associated with the decomposition of HOA to TCP.

A good agreement was found between the decomposition of HOA to TCP (or  $\alpha_{\text{HOA}}$ ) and liberation of water (or  $\alpha_{\text{H}_2\text{O}}$ ). It is assumed that at temperatures lower than 1673 K the thermal energy was not sufficient for activating the diffusion of water towards the surface of sintered HOA ceramic material. An equilibrium was established between HOA and H<sub>2</sub>O (cf. reaction 13) and the decomposition of HOA stopped. At higher temperature ( $\geq 1673$  K), HOA started to decompose to TCP. The defects in the HOA lattice and its transformation to the TCP lattice, as well as the surfaces at the grain boundaries allowed the water to be released during the second stage of decomposition. The decomposition of HOA ceramic material to TCP started on the surface at the points of defects, pores and grain boundaries (HOA). The TCP grains first coated the entire surface of the sintered ceramic material and only then its thickness started to grow. Unlike the case described in [17], no TCP grains were found inside the HOA ceramic material.

The time dependence of layer thickness was described by the parabolic law [13]. The experimental curve deviated from the theoretical one at the beginning of the thermal exposure when the entire surface was still not coated with the TCP layer. Once the products covered the whole surface, the agreement became satisfactory. Diffusion of water towards the surface was the rate determining step for the thermal decomposition of HOA and TCP. Qualitative phase analysis of HOA decomposition products and kinetic analysis by means of the J-M-A-J-K equation proved that the decomposition of HOA to TCP proceeded by a diffusion process.

The exponent factor evaluated from the J-M-A-J-K equation for the temperature interval of 1673–1758 K had the value of 0.5 to 0.53. This value corresponds to the diffusion mechanism of the decomposition [16]. However, the diffusion mechanism of decomposition holds only for sintered HA ceramics.

The kinetic analysis of thermal decomposition of powdered HA yielded an exponent factor of 0.59 to 0.65. The values show that the rate of thermal decomposition of powdered HA is controlled not only by diffusion of water, but also by formation of nuclei of the newly arising TCP phase.

## 5. Conclusion

Thermal decomposition of injection-moulded HA ceramics over the temperature range of 1473–1758 K involved three processes: sintering of HO (HOA) ceramics, separation of water and conversion of HA to HOA, and decomposition of HOA to TCP. In the course of sintering, HA lost 40 to 50% H<sub>2</sub>O and was transformed to HOA. The decomposition of HOA to TCP took place over the temperature range of 1673–1758 K.

The decomposition of HOA started on the sample surface. At first, individual TCP grains were formed and then a continuous layer of the reaction product (TCP). The increase in thickness of the TCP layer was described by the exponential law holding for diffusion processes. Kinetic analysis by means of the J-M-A-J-K equation likewise showed that the rate of HOA-TCP conversion was controlled by diffusion of water towards the surface of the sintered material. The activation energy of decomposition of HOA ceramics was found to amount to 283.5 kJ/mol.

### Acknowledgement

This study was supported by EC grant CIPA-CT94-0233 and CZ grants VS96121 and GA106/95/0359. The authors express their thanks to Mrs. D. Janova for SEM measurements.

### References

1. J. CIHLAR and M. TRUNEC, *Biomaterials* **17** (1996) 1905.
2. *Idem.*, in "Proceedings of the 10th International Symposium on Bioceramics in Medicine, Paris, 1997," edited by L. Sedel and C. Rey (Elsevier, Oxford, 1997), p. 183.
3. R. Z. LEGEROS, J. P. LEGEROS, Y. KIM, R. KIJKOWSKA, R. ZHENG, C. BAUTISTA and J. L. WONG, in "Bioceramics: Materials and Applications," edited by G. Fischman, A. Clare and L. L. Hench (American Ceramic Society, Ohio, 1995), p. 173.
4. R. Z. LEGEROS, *Clin. Mat.* **14** (1993) 65.
5. T. KIJIMA and M. TSUTSUMI, *J. Amer. Ceram. Soc.* **62** (1979) 455.
6. J. C. TROMBE and G. MONTEL, *Compt. Rend. Acad. Sci. SerC* **273** (1971) 462.
7. A. RAVAGLIOLI and A. KRAJEWSKI, "Bioceramics" (Chapman and Hall, London, 1992), p. 57.
8. B. LOCARDI, V. E. PAZZAGLIA, C. GABBI and B. PROFILO, *Biomaterials* **44** (1993) 437.
9. R. Z. LEGEROS and J. P. LEGEROS, in "An Introduction to Bioceramics," edited by L. L. Hench and J. Wilson (World Scientific, Singapore, 1993), p. 139.
10. S. GOTTSCHLING, R. KOHL, A. ENGEL and H. J. OEL, in "Bioceramics: Materials and Applications," edited by G. Fischman, A. Clare and L. Hench (American Ceramic Society, Ohio, 1994), p. 201.
11. R. JENKINS (and others editors): in "Powder Diffraction File, Inorganic Phases" (JCPDS International Centre for Diffraction Data, Swarthmore, 1987).
12. H. P. KLUG and L. E. ALEXANDER, *X-Ray Diffraction Procedures for Polycrystalline and Amorphous Materials* (Wiley, New York, 1974).
13. S. F. HULBERT, *J. Brit. Ceram. Soc.* **1** (1970) 11.
14. J. ŠESTÁK, V. ŠATAVA and W. W. WENDLANDT, *Thermoch. Acta* **13** (1973) 333.
15. C. H. BAMFORD and C. F. H. TIPPER, in "Comprehensive Chemical Kinetics, Vol. 22" (Elsevier, Amsterdam, 1980) p. 71.
16. *Idem.*, in "Comprehensive Chemical Kinetics, Vol. 22" (Elsevier, Amsterdam, 1980) p. 69.
17. A. ROYER, J. C. VIGUIE, M. HEUGHEBAERT and J. C. HEUGHEBAERT, *J. Mater. Sci.: Mater. in Medicine* **4** (1993) 76.

Received 4 April 1998

and accepted 9 April 1999